VII International Conference on Computational Methods in Marine Engineering
MARINE 2017
M. Visonneau, P. Queutey and D. Le Touzé (Eds)

FLOW STUDY ON A DUCTED AZIMUTH THRUSTER

PATRICK SCHILLER*, KEQI WANG* AND MOUSTAFA ABDEL-MAKSOUD*

* Institute for Fluid Dynamics and Ship Theory (M-8), Hamburg University of Technology,
Am Schwarzenberg-Campus 4, 21073 Hamburg, Germany
e-mail: patrick.schiller@tu-harburg.de, url: http://www.tuhh.de/fds

Key words: Computational Methods, Marine Engineering, Ducted Azimuth Thruster

Abstract. This paper presents the results of the numerical validation and verification studies on an azimuth thruster. The numerical investigations include a grid study as well as an analysis of the simulation results obtained by different isotropic an anisotropic turbulence models, such as k-omega, SST, SAS-SST, BSL-EARSM and DES. The numerical simulation results of selected flow conditions are compared with experimental data. To investigate scale effects on the open water results numerical computations are carried out for a thruster in full- and model scale and the calculated thrust and torque coefficients are compared with model scale simulations and measurements.

1 INTRODUCTION

Azimuth Thrusters may experience considerable high dynamic loads due to operation in extreme off-design conditions. The flow on Azimuth Thrusters is highly unsteady due to large cavitation and separation areas, which may take place at strong oblique flow conditions. These strong oblique flows can be caused by high steering angles of the azimuth thruster, due to high drift angle of the ship or strong ocean currents. This may lead to high continuous changes in the amplitudes of the forces and moments and to flow separation on propeller blades and other components of the propulsion system, such as the shaft, the connecting struts between the nozzle and propeller hub or to the gondola.

The hydrodynamic behaviour of an azimuth thruster is studied within a Norwegian and German research project called Inter-Thrust. The project is carried out within the framework of MARTEC-II network under the lead of MARINTEK and participated by Havyard Ship Technology, Voith Turbo GmbH, Jastram GmbH and Hamburg University of Technology. In a first stage in the project different CFD modelling approaches with respect to grid resolution and turbulence modelling are investigated and subjected to validation and verification studies on a number of selected cases.

Advanced numerical methods based on the Navier-Stokes equations are particularly efficient in the simulation of the complex unsteady flow on ship propulsion systems such as nozzle propellers or POD drives [4][5]. In combination with multi-scale turbulence, e.g. Hybrid RANS-LES methods, CFD methods are capable of resolving strongly unsteady vortical structures in separated flow areas [6].

The validation and verification work has the purpose to develop best practice approaches regarding computation mesh, modeling of turbulence, and feasibility of engineering calculations over a large matrix of cases. Therefore, the validation and verification studies are

started with four simplified cases, for which detailed experimental data exist.

2 OBJECT OF INVESTIGATION

The investigated azimuth thruster is designed by MARINTEK. It was used at MARINTEK for experimental studies under various operation conditions. Thus, a lot of validation data is available. Figure 1 shows the thruster configuration.

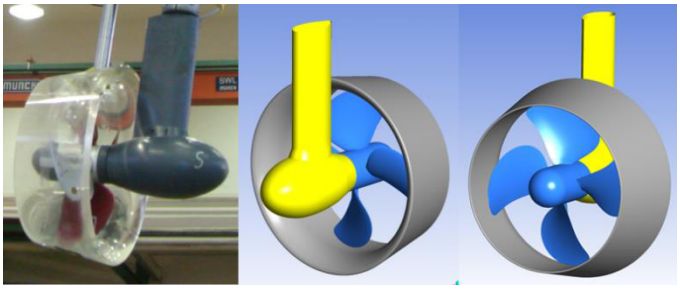

Figure 1: Model thruster configuration, experimental (left) and CAD (middle and right).

The thruster housing, shaft and gondola, have a generic geometry and are manufactured in PVC. The model duct D-136 is used during the tests. This duct is of 19A type without diffuser. The duct is made of Plexiglas and has a length of 125 mm and is centered at propeller plane. The main specification of the duct is given in Table 1. The P-1374 model propeller is used in this thruster configuration and has also generic geometry designed by MARINTEK. The four-blade right-handed propeller can be used as ducted and open propeller and is made of aluminium alloy. Table 1 contains the main specification data of the propeller.

Table 1: Main specifications of propeller (left) and duct (right).

Propeller diameter	250 mm
Hub diameter	60 mm
Design pitch ratio	$P_{r/R=0.7}$/D 1.1
Skew	25 degrees
Expanded blade area ratio	0.6

Duct Length	125 mm
Inner duct diameter	252.78 mm
Max. outer duct diameter	303.96 mm
Duct leading edge radius	2.78 mm
Duct trailing edge radius	1.39 mm

3 NUMERICAL METHODE

For this work, all numerical simulations are performed with the commercial CFD code ANSYS CFX (Release Version 15.0). It is a RANS method for steady and unsteady cases which numerically solves the unsteady equations of mass and momentum conservation:

$$\frac{\partial \rho}{\partial t} + \nabla \cdot (\rho U) = 0 \tag{1}$$

$$\frac{\partial (\rho U)}{\partial t} + \nabla \cdot (\rho U \otimes U) = -\nabla p + \nabla \cdot \tau + S_M \tag{2}$$

Where the stress tensor, τ, is related to the strain rate by:

$$\tau = \mu \left(\nabla U + (\nabla U)^T - \frac{2}{3} \rho \nabla \cdot U \right) \tag{3}$$

The ANSYS CFX solver uses second order discretization by default and is optimized for

high performance computing. Different turbulence closure models (e.g. SST, SAS, DES and LES) are available. Free surfaces are handled via VOF based formulation and cavitation models based on Euler-Euler formulations are also available. For more details see [1].

4 SIMULATION CONDITIONS

4.1 Simulation Domain and Numerical Grid

All numerical grids are generated with ANSYS ICEM CFD meshing software. The computational domain consists of three parts:

- rotating propeller domain,
- thruster domain which includes the whole thruster geometry. The domain has a cylindrical shape and can be rotated around a vertical rotation axis of the thruster,
- exterior area.

The thruster domain has a diameter of 4D and a height of 3D. The exterior area has a quadratic form of 14D x 14D and a height of 7D. Figure 1 shows the used domain arrangement. For the consideration of different inflow angles towards the thruster the exterior area can be rotated. The free surface is neglected and the top of the domain is treaded as free slip wall. Except the in- and the outlet, the other boundaries are threaded as openings. The boundaries of the three domains are connected by sliding interfaces.

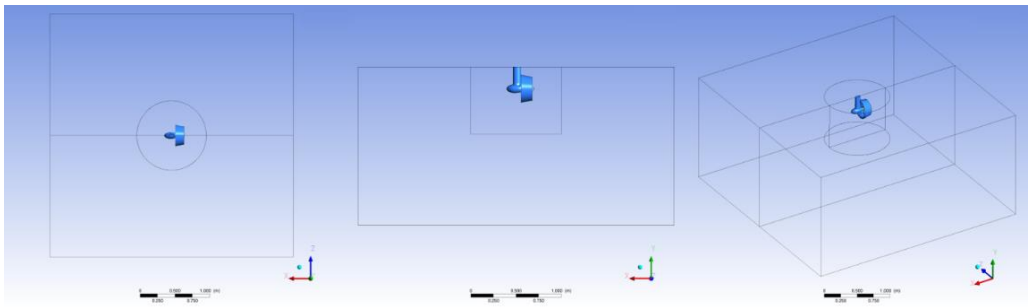

Figure 2: Computational domain arrangement: top view, side view and perspective view.

Table 2: Cell numbers for the different grids.

Grid No. / Domain part	Number of cells			
	Propeller	Thruster	Exterior area	Total
Grid 1 (2.7M)	1.42 M	0.99 M	0.29 M	2.70 M
Grid 2 (6M)	3.59 M	2.37 M	0.29 M	6.25 M
Grid 3 (20M)	11.92 M	7.23 M	0.29 M	19.44 M
Grid 4 (53M)	30.88 M	21.88 M	0.29 M	53.05 M
Grid 5 (27M)	11.62 M	14.11 M	1.63 M	27.36 M

Various structured grids with different characteristics have been generated, see Table 2. Grid number 1 to 4 are used for a grid study, whereby grid number 5 is generated for DES simulations, because they need a finer and more adapted grid regarding cell size and aspect ratio. The four meshes for the grid study follow a refinement factor of $1/\sqrt{2}$ in each spatial direction of the propeller and thruster domain. The cell number of the exterior area is kept

constant. Details of the grid arrangement can be seen in Figure 3. The Y^+ value is ≈ 1 for grid 3.

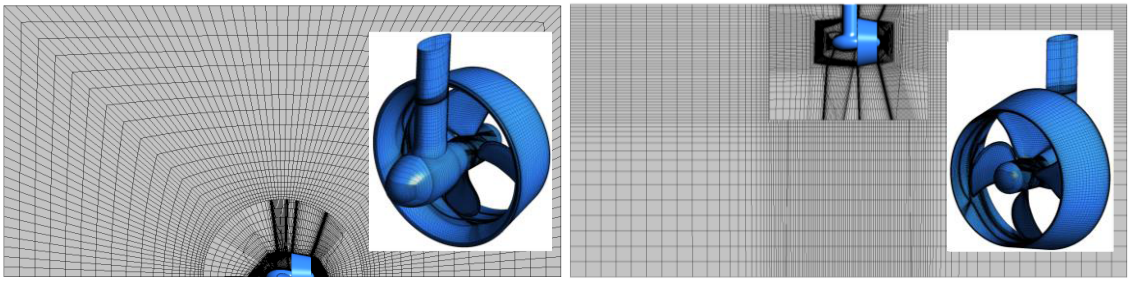

Figure 3: Details of the numerical grid, exemplary for grid 2.

4.2 Flow Conditions

Four different operating conditions of the ducted thruster are considered for the grid study and the investigation of the performance of the different turbulence models. The conditions correspond to experiments performed at MARINTEK. The cases are characterized by the advance ration J, the rotational number of the propeller n and the heading angle β of the thruster, as listed in Table 3.

Table 3: Overview on used flow conditions.

Case No.	J [-]	n [rps, Hz]	Head. Angle β [deg]
1	0.0	9	0
2	0.6	11	0
3	0.6	9	-35
4	0.6	9	+35

For the validation of the of the open water characteristics additionally the following J-values at n=11Hz are simulated: J=0.15; 0.3; 0.45; 0.75; 0.85; 0.95 and 1.05. For the full-scale version, the same J-value are considered. The scaling factor is 20 and gives a propeller diameter of D=5m. The rotational speed of the propeller is n=2.46Hz for full-scale.

4.3 Turbulence Models

For all four operating conditions simulation are performed with different turbulence closure models. Following turbulence models have been used from ANSYS CFX:

- k-omega
- SST (as default)
- SAS-SST
- BSL-EARSM
- DES

The first two models (k-omega and SST) are isotropic models where the eddy viscosity is the same in each spatial direction. Whereas the other used models are anisotropic. For further details regarding the turbulence models see [1].

For the simulation with the DES model grid 5 has been generated, as mentioned before. This is due to the higher requirements regarding the cell sizes and aspect ratios for this turbulence model. For all other turbulence models grid 3 (20M cells) is used. The result from the SST model is used as initialization for the simulations with the SAS-SST, the BSL-EARSM and the

DES turbulence model.

4.4 Simulation Setup

In all simulations the timestep is set to 4° propeller rotation, except the simulations with the SAS-SST and DES turbulence model, here a timestep for 1° propeller rotation is used. For each timestep four inner iterations are considered. Several propeller revolutions are simulated till a periodic solution (quasi-steady) behaviour is achieved.

5 EVALUATION

For comparison with the experimental results obtained by MARINTEK different force and moment coefficients are calculated in a thruster fixed coordinate system for the propeller, the duct and the whole propulsion unit. The following values are evaluated:

- kt Propeller (KTP) Propeller Thrust
- 10kq Propeller (10KQP) Propeller Torque
- kt Duct (KTD) Thrust of Duct
- kt Total (KTTOT) Total Thrust of the Unit
- kside Duct (KDS) Side Force of Duct
- kside Total (KSTOT) Total Side Force of the Unit
- 10kMz (10KMZ) Steering Moment (only shaft, gondola and propeller)

From the quasi steady solution result of each simulation an average over the last 1, 2 and 4 propeller revolution is calculated and normalized. The forces and moments are normalized as usual:

Forces by $rho * n\text{^}2 * D\text{^}4$ (4)

Moments by $rho * n\text{^}2 * D\text{^}5$ (5)

Additionally, a verification and validation (V&V) analysis [3] for the above mentioned values is carried out. The error (E) between CFD (S) and EFD (D) is expressed by following formula:

$$|\mathrm{E}(\%\mathrm{D})| = \left|\frac{\mathrm{S}-\mathrm{D}}{\mathrm{D}} \times 100\right| \quad (6)$$

6 SIMULATION RESULTS

Before the simulations results are analysed in detail some aspects should be mentioned. The first point is that for measuring the duct thrust in the model tests a separate shaft is used to connect the duct to the force balance. This shaft is not included in the thruster geometry considered in the numerical simulations, see Figure 1. This affects the mainly the total forces from the duct especially those at $\beta = \pm 35°$.

A second point is that in the measurements the magnitude of the steering moment (10KMZ) at $\beta = \pm 35°$ is quite differently, but one would expect values in the same order of magnitude. The simulation results as well as in other experimental investigations with the same thruster configuration without duct [2] (Fig 8) indicate that the steering moment is nearly symmetric for

both sides. So, there might be a problem in the measurements concerning the value for at β = +35°. Also, the values of the steering moment are quite small due to the well-balanced shaft, gondola and propeller arrangement.

6.1 Open water characteristics

As mentioned above, simulations are performed to determine the open water characteristic of the selected azimuth thruster unit and to compare them with the experimental results. Grid 2 (6M) is used and the thruster is simulated at above mentioned 7 J-values in model (MS) and in a full-scale (FS) version. The simulation results can be found in Figure 4 a-f.

The propeller thrust as well as the propeller torque (Figure 4 a and b) of the model scale variant agree very well with the experimental values. The KTP and 10KQP values for the full-scale are slightly smaller at low J-values and higher at huge J-values.

Regarding the duct thrust (Figure 4 c) the model scale values agree well in the range of J = 0.15 to 0.75 with the experimental. For J = 0 the value is slightly below the experiments whereas for J-values greater than 0.75 the values are clearly above. The values for the full-scale version separate from the experimental ones from J = 0.6 and the distance to greater values grows. The differences between the three curves at high J-values come from different flow separation areas at the leading edge of the duct as indicated in Figure 7.

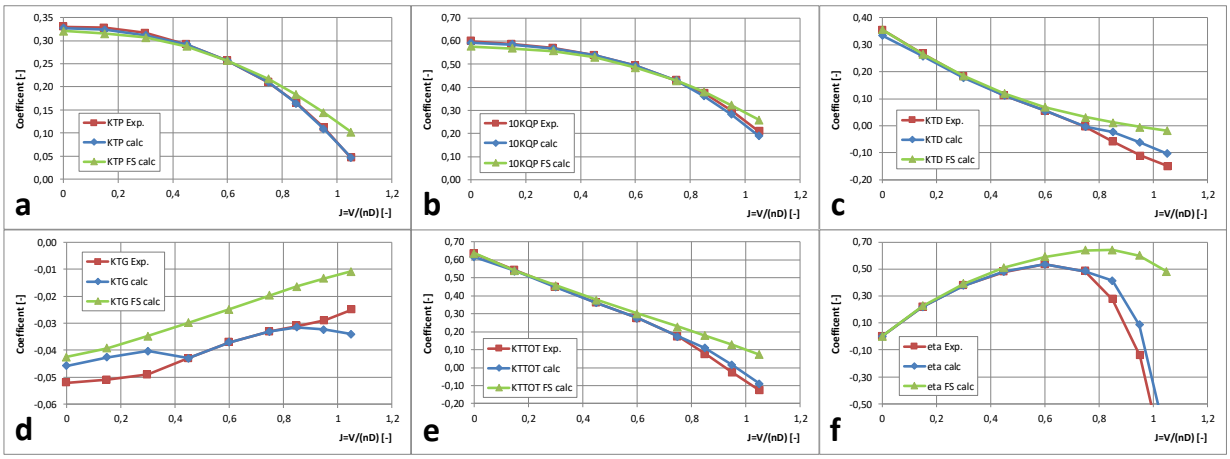

Figure 4: Comparison over different advance ratios of a) propeller thrust (KTP); b) propeller torque (KQP) c) duct thrust (KTD); d) housing resistance (KTG); e) total thrust (KTTOT) and f) thruster efficiency (eta).

Figure 4 d shows the comparison of the housing resistance (shaft + gondola). Here the three curves are quite differently but the general trend shows a lower resistance with increasing J-values. The full-scale variant has the lowest drag. The experimental curve has the same tendency as the full-scale version but shifted to higher drag values. The calculated values for model scale are till J = 0.45 lower than the experimental ones. From J = 0.45 to 0.95 they are almost identical and after that they are higher. These differences might come from differently predicted flow separation area due to not sufficient mesh resolution in this region.

The comparison of the total trust produced by the whole thruster unit can be found in Figure 4 e. The value for the three curves are till J = 0.6 almost identical. Beyond that the full-scale variant shows higher value due to the higher duct thrust. This can also be seen in the total

thruster efficiency illustrated in Figure 4 f. Here the full-scale version reaches the highest efficiency over a greater range.

Further the scale effects between the calculated model scale and the full-scale thruster version are analysed. The differences ($\Delta = (FS - MS)/MS * 100\%$) are presented in Figure 5 a-e for the different coefficients. The scale effects on the propeller thrust und torque (Figure 5 a and b) show in general the same trend. The coefficients are lower for full scale which leads to a negative difference. These increases slightly till J = 0.15 and then continuously decreases. The differences are greater for the propeller torque so that this results in a better efficiency for the full-scale version in total. A comparison of the pressure distribution and limiting streamlines on the propeller at J = 0 and J = 0.6 can be found in Figure 6 left. Clearly visible is that the flow in the model scale case cannot provide enough shear force against centrifugal force; hence the streamlines on both blade sides are not travelling along the circumferential direction but through the various radii.

Figure 5 c illustrates the scale effect regarding the duct thrust. The difference is positive indicating a greater thrust for FS and lies around about 5% till J =0.45. Beyond that the delta increases rapidly to value over 20% because the produced thrust of the duct in MS at high J-values becomes small and even negative. As mentioned before the differences at high J-values come from different flow separation regions at the leading edge of the duct as indicated in Figure 7.

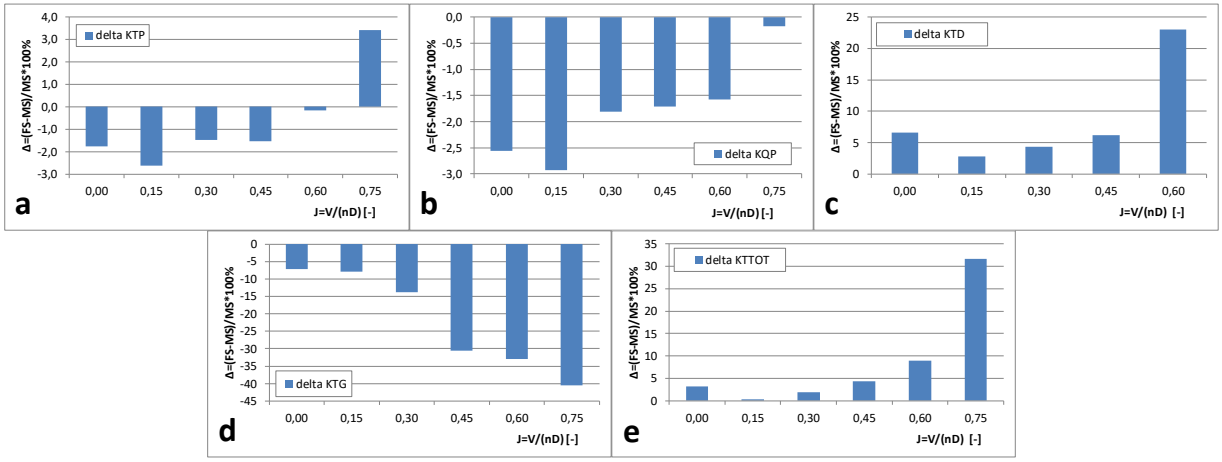

Figure 5: Scale effects for different advance ratios on a) propeller thrust (KTP); b) propeller torque (KQP) c) duct thrust (KTD); d) housing resistance (KTG) and e) total thrust (KTTOT)**.**

The scale effect regarding the housing resistance, depicted in Figure 5 d, is continuously increasing from about 7% at J =0 to 40% at J = 0.75. The difference is negative which means that the resistance is lower for the full-scale version. This increasing scale effect is caused mainly by separation effects on the shaft. Figure 6 right show the pressure distribution and limiting streamlines on the shaft and the gondola where this fact is explicit visible. The separation zone is in FS smaller than in MS which leads to a smaller resistance. The flow separation is induced by the high positive pressure gradient in this region. Due to the higher suction impact of the propeller at low J-values the separation zones are smaller at low inflow velocities.

With respect to the total thrust produced be the azimuth thruster (Figure 5 e) one can see

after a slight reduction at J = 0.15 a progressive increasing scale effect with increasing J-value. This mainly caused by the greater duct and propeller thrust in full-scale.

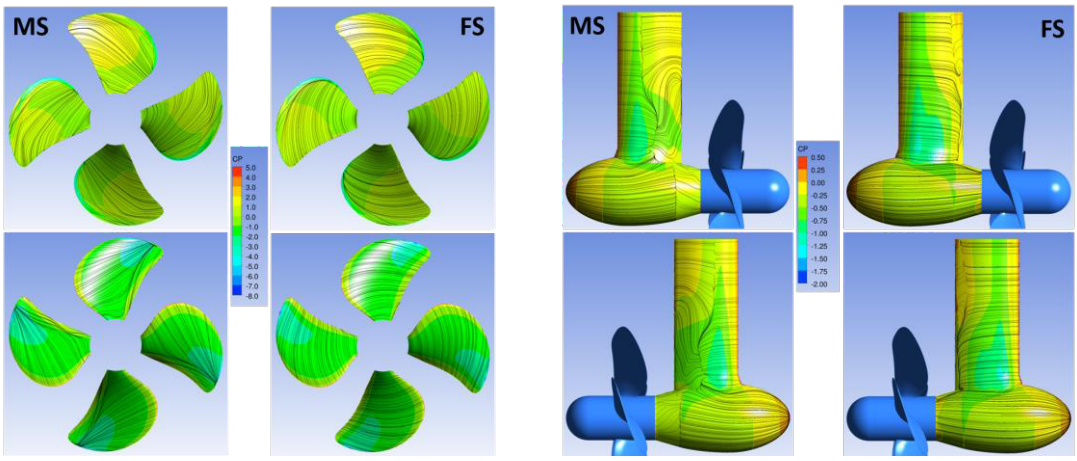

Figure 6: Pressure distribution and streamlines on the propeller blades (left, top row pressure side and bottom row suction side) and the housing (right) at J=0.6 and β=0°, comparison model scale vs. full scale.

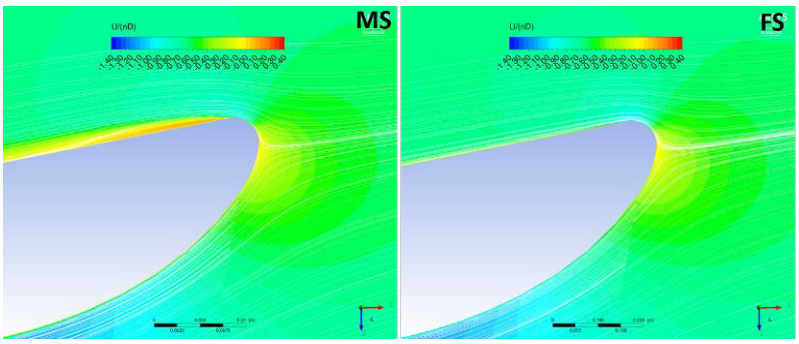

Figure 7: Flow details around the duct at J=0.6 and β=0°.

6.2 Validation

The validation and verification work has the purpose of development of best practice approaches regarding computation mesh resolution, modelling of turbulence, and feasibility of engineering calculations over a large matrix of cases. Therefore, the validation and verification studies are started with four simplified cases, for which detailed experimental data exist.

Grid resolution

All four above described cases are calculated on grid 1 to 4. The maximal occurred Y+-value for all investigated flow conditions during the simulation is 7, 5, 3.5 and 2.5 for grid 1, 2, 3 and 4 respectively. The calculated coefficient values for case 1 to 4 can be found in the Table 4 to Table 7. Also, the error of the simulation values with respect to the experimental ones are shown in the tables.

For case 1 and 2 the propeller thrust and torque coefficients agrees very well for all grid resolutions with respect to the experimental ones. They lie in-between a deviation of maximal 2%. The thrust coefficient of the duct is in case 1 underpredicted by 4-8%, whereby the difference decreases with higher mesh resolution. Whereas the duct thrust is overpredicted

about 12-16% in case 2. The deviation is for the grids 2,3 and 4 nearly the same. A possible reason for this high deviation might be the missing resistance from the mounting of the duct to the force balance in the computation. Because of the variation in the duct thrust the same tendencies can be found in the total thrust of unit. The deviation is 1-4% below the measured values for case 1 and 2-6% above for case 2.

Due to the heading angle of $\beta = 0°$ for case 1 and 2 the duct and total unit side force coefficients are very small. The small values of the forces can lead to large deviations which is here the case. Therefore, the values are not further assessed here.

Table 4: Simulation results of grid resolution study for case 1, J=0.0, n=9Hz, β =0°.

	Setup	kt Propeller	10kq Propeller	kt Duct	kt Total	kside Duct	kside Total	10M Total
Coefficients	Experiment	0.3300	0.6000	0.3560	0.6340	0.0030	-0.0130	0.0150
	2.7 M SST	0.3288	0.5955	0.3268	0.6101	0.0015	0.0035	0.0182
	6 M SST	0.3269	0.5921	0.3350	0.6162	0.0016	0.0030	0.0222
	20 M SST	0.3278	0.5936	0.3395	0.6214	0.0008	0.0030	0.0204
	53 M SST	0.3308	0.5998	0.3427	0.6273	0.0008	0.0033	0.0176
Errors	2.7 M SST	-0.4	-0.8	-8.2	-3.8	-50.0	-126.8	21.0
	6 M SST	-0.9	-1.3	-5.9	-2.8	-48.1	-122.9	48.1
	20 M SST	-0.7	-1.1	-4.6	-2.0	-72.7	-123.2	36.1
	53 M SST	0.2	0.0	-3.7	-1.1	-72.2	-125.8	17.5

Table 5: Simulation results of grid resolution study for case 2, J=0.6, n=11 Hz, β =0°.

	Setup	kt Propeller	10kq Propeller	kt Duct	kt Total	kside Duct	kside Total	10M Total
Coefficients	Experiment	0.2570	0.4930	0.0560	0.2760	0.0000	-0.0130	0.0200
	2.7 M SST	0.2548	0.4882	0.0628	0.2828	0.0016	0.0045	0.0114
	6 M SST	0.2573	0.4934	0.0652	0.2877	0.0021	0.0042	0.0139
	20 M SST	0.2585	0.4964	0.0649	0.2904	0.0029	0.0040	0.0159
	53 M SST	0.2590	0.4982	0.0651	0.2926	0.0027	0.0032	0.0187
Errors	2.7 M SST	-0.9	-1.0	12.2	2.5		-134.7	-42.9
	6 M SST	0.1	0.1	16.5	4.3		-131.9	-30.5
	20 M SST	0.6	0.7	15.9	5.2		-130.9	-20.3
	53 M SST	0.8	1.0	16.3	6.0		-124.5	-6.6

Table 6: Simulation results of grid resolution study for case 3, J=0.6, n=9 Hz, β =-35°.

	Setup	kt Propeller	10kq Propeller	kt Duct	kt Total	kside Duct	kside Total	10M Total
Coefficients	Experiment	0.2020	0.4060	0.1280	0.3010	0.2820	0.4110	-0.0520
	2.7 M SST	0.1973	0.4072	0.1212	0.3308	0.2504	0.3828	0.0195
	6 M SST	0.2130	0.4189	0.1350	0.3146	0.2576	0.3705	-0.0476
	20 M SST	0.2114	0.4175	0.1368	0.3085	0.2533	0.3567	-0.0632
	53 M SST	0.2124	0.4191	0.1375	0.3036	0.2551	0.3703	-0.0567
Errors	2.7 M SST	-2.3	0.3	-5.3	9.9	-11.2	-6.9	-137.5
	6 M SST	5.5	3.2	5.5	4.5	-8.7	-9.8	-8.4
	20 M SST	4.6	2.8	6.9	2.5	-10.2	-13.2	21.5
	53 M SST	5.2	3.2	7.4	0.9	-9.5	-9.9	9.1

Table 7: Simulation results of grid resolution study for case 4, J=0.6, n=9 Hz, β =+35°.

	Setup	kt Propeller	10kq Propeller	kt Duct	kt Total	kside Duct	kside Total	10M Total
Coefficients	Experiment	0.3000	0.5420	0.1640	0.4280	-0.3050	-0.4470	0.0080
	2.7 M SST	0.2907	0.5645	0.1553	0.4638	-0.2562	-0.3801	-0.0072
	6 M SST	0.2937	0.5489	0.1601	0.4256	-0.2497	-0.3373	0.0525
	20 M SST	0.2949	0.5529	0.1684	0.4295	-0.2708	-0.3636	0.0689
	53 M SST	0.2992	0.5601	0.1695	0.4312	-0.2692	-0.3646	0.0687
Errors	2.7 M SST	-3.1	4.1	-5.3	8.4	-16.0	-15.0	-189.7
	6 M SST	-2.1	1.3	-2.4	-0.6	-18.1	-24.5	555.7
	20 M SST	-1.7	2.0	2.7	0.4	-11.2	-18.7	761.0
	53 M SST	-0.3	3.3	3.3	0.7	-11.7	-18.4	758.7

Also, due to the well-balanced shaft, gondola and propeller arrangement small steering moment values are calculated, see the results of case 1 and 2. In both cases the quality of the steering moment results is improved significantly with increasing grid resolution.

The deviation of the coefficients for propeller thrust and torque, duct thrust as well as total thrust of the unit in general lie for the cases 3 and 4 in a range of max. ±5%. The largest

deviation can be found in the case of grid 1 with the lowest cell number. The other three grids show nearly the same deviations. For case 3 the predicted values are in general slightly larger, whereas the values for case 4 are slightly smaller, particularly the values of the propeller thrust.

The calculated values for the side forces (duct and total) are underpredicted. The deviations to the experiment is around 10-20%, whereas the deviations are a bit higher for case 4. Keeping in mind that the duct mounting connection to the force balance, which creates additional side force, is missing in the simulation, the prediction accuracy seems to be within acceptable range. No clear trend is recognizable regarding the mesh resolutions for grid 2, 3 and 4 because the deviations lie in the same range.

This is not the case at least for the deviation of the steering moment at case 3. Here the accuracy of the predicted results gets higher with finer mesh resolution. The smallest deviation is 9% at grid 4. For case 4 it is difficult to conclude a clear statement. As mentioned above the measured value might be defective which leads to very high and illogical deviations.

Turbulence Models

All four flow cases are calculated with the above mentioned turbulence models. Except for the DES model, where grid 5 is employed, grid 3 is used. The calculated coefficient values for case 1 to 4 can be found in the Table 8 to Table 11. Again, the errors between the simulation and the experiments are shown in the tables.

For case 1 and 2 the propeller thrust is well predicted by all applied turbulence models within a deviation of 1% with the exception of the k-omega and DES model where the deviation is up to 3%. Also, the propeller torque is very well predicted for case 1 and 2 by all turbulence models without any exception. The deviation lies here in a range of 1%.

All turbulence models underpredict the duct thrust for case 1 by about 5 % and overpredict it for case 2 by about 14%. This deviation is quite high, but acceptable due to the missing consideration of the mounting resistance of the duct in the computation. Because the total thrust of the unit is composed mainly of the propeller and duct thrust the same tendencies can be found here. The deviation is 2-4% below the measured values for case 1 and 2-5% above for case 2.

Due to the fact that for case 1 and 2 the values of the duct and total unit side force as well as for the steering moment are very small, the deviations are quite large. Also, no clear trend can be found regarding the turbulence modelling. Therefore, the values are not further assessed here.

For the cases with $\beta=\pm35°$ heading angle the propeller thrust is overpredicted about 3-6% for case 3 and underpredicted about 2-6% for case 4. Again, the k-omega and DES model show slightly smaller thrust coefficients than the other models. The propeller torque is predicted by all turbulence models quite well for both cases (3 and 4). The deviation is 2-5% above the measured ones.

The deviation for the duct trust is 3-7% above the experimental values for case 3 and around 2-3% for case 4. Also, here the k-omega and DES model show slightly smaller duct thrust coefficients than the other models. Due to the marginally over predicted propeller and duct thrust for case 3 also the total thrust is overpredicted by 3-8%. For case 4 the prediction quality is better and the deviation is below 2% because of the underpredicted propeller thrust.

The calculated values for the duct and total side forces are comparably underpredicted by all turbulence models. The deviations to the experiment is around 10-12% for the duct side force and 14-20% for the total side force. For case 4 the deviations are a bit higher than for case 3.

As mentioned above due to the missing duct mounting in the simulation, a validation of the total side force is not possible.

The prediction of the steering moment at case 3 shows a clear picture regarding the turbulence modelling. Here the k-omega and DES model significantly under predict the steering moment. The deviation is at least 25%. The other models overpredict the by 14-21%. For case 4 it is difficult to make a clear statement, as the measured value might be defective.

Table 8: Simulation results of turbulence model variation for case 1, J=0.0, n=9Hz, β =0°.

	Setup	kt Propeller	10kq Propeller	kt Duct	kt Total	kside Duct	kside Total	10M Total
Coefficients	Experiment	0.3300	0.6000	0.3560	0.6340	0.0030	-0.0130	0.0150
	20 M SST	0.3278	0.5936	0.3395	0.6214	0.0008	0.0030	0.0204
	20 M k-omega	0.3200	0.5996	0.3319	0.6089	0.0025	0.0053	0.0253
	20 M BSL-EARSM	0.3283	0.5948	0.3388	0.6218	0.0034	0.0048	0.0235
	20 M SAS-SST	0.3282	0.5946	0.3389	0.6213	0.0121	0.0176	-0.0280
	27 M DES	0.3197	0.5940	0.3371	0.6136	0.0108	0.0142	-0.0206
Errors	20 M SST	-0.7	-1.1	-4.6	-2.0	-72.7	-123.2	36.1
	20 M k-omega	-3.0	-0.1	-6.8	-4.0	-18.2	-141.1	68.7
	20 M BSL-EARSM	-0.5	-0.9	-4.8	-1.9	12.9	-136.6	56.9
	20 M SAS-SST	-0.5	-0.9	-4.8	-2.0	302.2	-235.3	-286.7
	27 M DES	-3.1	-1.0	-5.3	-3.2	260.0	-209.1	-237.3

Table 9: Simulation results of turbulence model variation for case 2, J=0.6, n=11Hz, β =0°.

	Setup	kt Propeller	10kq Propeller	kt Duct	kt Total	kside Duct	kside Total	10M Total
Coefficients	Experiment	0.2570	0.4930	0.0560	0.2760	0.0000	-0.0130	0.0200
	20 M SST	0.2585	0.4964	0.0649	0.2904	0.0029	0.0040	0.0159
	20 M k-omega	0.2497	0.4991	0.0609	0.2827	0.0013	0.0033	0.0132
	20 M BSL-EARSM	0.2589	0.4992	0.0636	0.2907	0.0027	0.0034	0.0104
	20 M SAS-SST	0.2599	0.4980	0.0634	0.2879	0.0048	0.0073	0.0104
	27 M DES	0.2508	0.4953	0.0605	0.2817	0.0027	0.0026	0.0135
Errors	20 M SST	0.6	0.7	15.9	5.2		-130.9	-20.3
	20 M k-omega	-2.9	1.2	8.8	2.4		-125.8	-34.2
	20 M BSL-EARSM	0.8	1.3	13.7	5.3		-126.2	-47.8
	20 M SAS-SST	1.1	1.0	13.2	4.3		-156.0	-47.8
	27 M DES	-2.4	0.5	8.1	2.1		-119.7	-32.4

Table 10: Simulation results of turbulence model variation for case 3, J=0.6, n=9 Hz, β =-35°.

	Setup	kt Propeller	10kq Propeller	kt Duct	kt Total	kside Duct	kside Total	10M Total
Coefficients	Experiment	0.2020	0.4060	0.1280	0.3010	0.2820	0.4110	-0.0520
	20 M SST	0.2114	0.4175	0.1368	0.3085	0.2533	0.3567	-0.0632
	20 M k-omega	0.2085	0.4284	0.1329	0.3258	0.2537	0.3639	-0.0248
	20 M BSL-EARSM	0.2136	0.4231	0.1358	0.3097	0.2458	0.3536	-0.0599
	20 M SAS-SST	0.2153	0.4207	0.1376	0.3105	0.2523	0.3547	-0.0592
	27 M DES	0.2105	0.4245	0.1327	0.3142	0.2533	0.3543	-0.0392
Errors	20 M SST	4.6	2.8	6.9	2.5	-10.2	-13.2	21.5
	20 M k-omega	3.2	5.5	3.9	8.2	-10.0	-11.5	-52.3
	20 M BSL-EARSM	5.7	4.2	6.1	2.9	-12.8	-14.0	15.3
	20 M SAS-SST	6.6	3.6	7.5	3.1	-10.5	-13.7	13.8
	27 M DES	4.2	4.6	3.6	4.4	-10.2	-13.8	-24.5

Table 11: Simulation results of turbulence model variation for case 4, J=0.6, n=9 Hz, β =+35°.

	Setup	kt Propeller	10kq Propeller	kt Duct	kt Total	kside Duct	kside Total	10M Total
Coefficients	Experiment	0.3000	0.5420	0.1640	0.4280	-0.3050	-0.4470	0.0080
	20 M SST	0.2949	0.5529	0.1684	0.4295	-0.2708	-0.3636	0.0689
	20 M k-omega	0.2816	0.5532	0.1606	0.4318	-0.2653	-0.3652	0.0459
	20 M BSL-EARSM	0.2934	0.5530	0.1644	0.4242	-0.2648	-0.3520	0.0544
	20 M SAS-SST	0.2962	0.5530	0.1686	0.4193	-0.2704	-0.3586	0.0794
	27 M DES	0.2835	0.5474	0.1595	0.4232	-0.2638	-0.3668	0.0595
Errors	20 M SST	-1.7	2.0	2.7	0.4	-11.2	-18.7	761.0
	20 M k-omega	-6.1	2.1	-2.1	0.9	-13.0	-18.3	473.5
	20 M BSL-EARSM	-2.2	2.0	0.2	-0.9	-13.2	-21.3	580.5
	20 M SAS-SST	-1.3	2.0	2.8	-2.0	-11.3	-19.8	892.3
	27 M DES	-5.5	1.0	-2.8	-1.1	-13.5	-17.9	644.2

7 CONCLUSIONS

In this work a generic azimuth thruster was investigated at different flow conditions. The

open water characteristics were calculated for model and full-scale configuration and compared with experimental values. Further a grid study with four different mesh resolutions was conducted for four diverse flow conditions. Finally, different isotropic and anisotropic turbulence models were compared for the four selected operating conditions.

The comparison of the calculated open water characteristics in model scale show in general a fair agreement with the measurement. Some deviations arise at high J-values probably due to not correctly captured separation phenomena on the duct and on the thruster shaft. Scale effects can be evaluated based on the calculated results of model and full-scale. Affected are mainly the duct thrust and the housing resistance due to separation phenomena particularly at high J-values. In total the scale effects lead to a higher efficiency over a larger advance ratio range for the full-scale version.

Regarding the results of the conducted grid study it can be said that the grids from and above 6M cells for the investigated operating conditions give good results. Also for "not complicated" flow conditions as for example for open water characteristic good results can be achieved on coarser grids, but partly and especially for the steering moment higher deviations can occur. Further it was ascertained that there is no significant accuracy increase with a finer grid resolution. The variation of the turbulence model has shown that no turbulence model is significantly better than another one for the here investigated azimuth thruster and flow conditions. All of them show a fair agreement with experimental results. This could be different if operating conditions are simulated with a huge amount of separated flow. The results of the k-omega and DES turbulence model reveal partly slightly lower coefficient values than the other ones.

In summary, the comparison of the simulation results with the model tests has shown that for the calculated cases of the investigated azimuth thruster a grid size of 6 to 10 million cells and the use of the SST turbulence model are sufficient to achieve reasonable accuracy at least for industrial applications. With finer grids and other turbulence models, partly slightly better results can be achieved, but they do not justify the considerably higher computational effort during a design stage.

8 REFERENCES

[1] ANSYS. Inc. *ANSYS CFX-Solver Theory Guide*. Release 15.0. November 2013

[2] Hamid Amini and Sverre Steen. *Experimental and Theoretical Analysis of Propeller Shaft Loads in Oblique Inflow*. Journal of Ship Research. December 2011

[3] Committee. A. V. *Standard for Verification and Validation in Computational Fluid Dynamics and Heat Transfer*. ASME. 2009

[4] Baltazar, J., Rijpkema, D., Falcao de Campos, J. A. C., *Bosschers, J.: A Com-parison of Panel Method and RANS Calculations for a Ducted Propeller System in Open-Water*, 3rd International Symposium on Marine Propulsors smp'13, 2013.

[5] Abdel-Maksoud, M., Heinke, H.-J.: *Scale Effects on Ducted Propellers*, 24th Symposium on Naval Hydrodynamics, 2002.

[6] Abbas, N., Kornev, N.: *Determination of the unsteady load of the propeller perfor-mance using hybrid RANS-LES methods*, STG Hamburg, 2014.